IEICE TRANSACTIONS

on Electronics

DOI:10.1587/transele.2024REP0002

Publicized:2024/09/10

This advance publication article will be replaced by the finalized version after proofreading.

A PUBLICATION OF THE ELECTRONICS SOCIETY

The Institute of Electronics, Information and Communication Engineers
Kikai-Shinko-Kaikan Bldg., 5-8, Shibakoen 3chome, Minato-ku, TOKYO, 105-0011 JAPAN

PAPER *Special Section on IEICE Transactions on Electronics*

Extended Kelvin Transformation for Solving Radiating Electromagnetic Fields*

Kengo SUGAHARA†, ***Member***

SUMMARY This paper presents an extension of the Kelvin transformation for high-frequency electromagnetic problems. The Kelvin transformation is a coordinate transformation that maps infinite space to a finite space, acting as a conformal transformation of Maxwell's equations. We apply concepts of differential geometry to derive the material constant's metric and spatial dependence in the exterior domain, which was originally proposed for low-frequency eddy current problems. This paper extends the conformal transformation concept to high-frequency problems by introducing a Perfectly Matched Layer (hereafter referred as to PML) in the exterior domain. This technique makes it easy to apply a simple Maxwellian PML.

key words: *Conformal transformation, finite element analysis, high frequency electromagnetic, Kelvin transformation, open boundary problems.*

1. Introduction

Electromagnetic field analysis, such as the finite element method (FEM) and the finite difference time domain method (FDTD), cannot directly handle open boundary problems. Various techniques have been developed to emulate them [1–24]. These techniques are called Asymptotic Boundary Conditions for low-frequency problems, where the effects of displacement currents are neglected, and Absorbing Boundary Conditions for high-frequency electromagnetic problems.

This paper focuses on one of these techniques, namely, the Kelvin transformation [11,12,14–19,25–29], which functions as an exact open boundary condition. The analysis domain is terminated by a circle for a two-dimensional problem or a sphere for a three-dimensional problem, and the exterior domain is Kelvin transformed and connected to the interior domain with unknown equivalent boundary conditions. In [29], the Kelvin transformation is reformulated to derive the conductivity, permittivity, and permeability in the exterior domain, conserving the conformal symmetry of Maxwell's equations [30]. The derived spatial functions of the material constants allow for materials in both the interior and exterior domains or even across the truncated boundaries.

This paper extends the idea of Extended Kelvin Transformtion [29] to high-frequency radiation problems, combined with the PML. The proposed method can be easily implemented to the conventional FEM solvers, withoud modifying the program.

For example, consider an antenna with multipath from mountains and buildings, as shown in Fig.1. If the analysis model includes the ground, buildings, and mountains, it becomes very large and requires a substantial computational cost. By applying the Extended Kelvin Transformtion with PML, we can limit the analysis domain to the region encompassing the antenna and include other scatterers in the exterior domain, by connecting the interior domain to the exterior domain with the unknown equivalent boundary contions. We validate the proposed method using a numerical computation model based on the FEM.

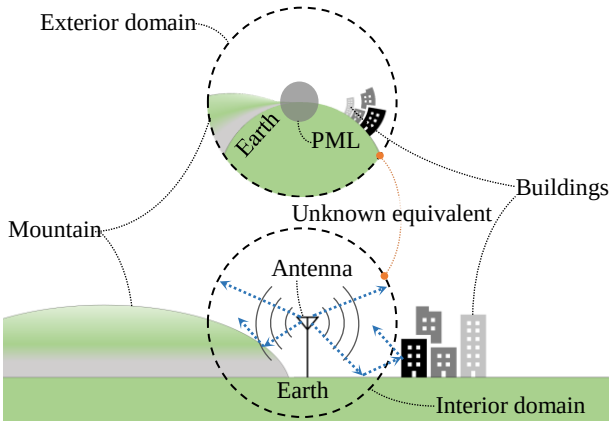

Fig. 1 Concept of the extended Kelvin transformation for high-frequency problems

2. Formulation

2.1 Deriviation of the Material Parameters in Exterior Domain

The basic idea of the Kelvin transformation for high-frequency problems is the similar to that proposed in reference [29] for low-frequency problems. The spacial coordinates of the Kelvin transformation in three-dimensions is given as (1) where x', y', and z' are exterior-domain coordinates and a is the radius of the interior-domain. The difference between low and high frequencies is that conversion to dielectric constant ϵ

†The author is with the Kindai University, Japan
*This paper was presented at ...

and magnetic conductivity σ^* in PML is required.

$$\begin{aligned} x' &= \left(\frac{a^2}{x^2+y^2+z^2}\right) x = \left(\frac{a}{r}\right)^2 x \\ y' &= \left(\frac{a^2}{x^2+y^2+z^2}\right) y = \left(\frac{a}{r}\right)^2 y \\ z' &= \left(\frac{a^2}{x^2+y^2+z^2}\right) z = \left(\frac{a}{r}\right)^2 z \end{aligned} \tag{1}$$

Line elements in spherical coordinate are given by (2).

interior domain	exterior domain
$h_r = 1$	$h'_r = -\dfrac{a^2}{r'^2}$
$h_\theta = r$	$h'_\theta = \dfrac{a^2}{r'}$
$h_\phi = r\sin\theta$	$h'_\phi = \dfrac{a^2}{r'}\sin\theta$

(2)

Surface elements in spherical coordinate are given by (3) where $r' = \sqrt{x'^2 + y'^2 + z'^2}$.

interior domain	exterior domain
$h_\theta h_\phi = r^2\sin\theta$	$h'_\theta h'_\phi = \dfrac{a^4}{r'^2}\sin\theta$
$h_\phi h_r = r\sin\theta$	$h'_\phi h'_r = -\dfrac{a^4}{r'^3}\sin\theta$
$h_r h_\theta = r$	$h'_r h'_\theta = -\dfrac{a^4}{r'^3}$

(3)

The magnefic field $\vec{\boldsymbol{H}}$(A/m), and electric field $\vec{\boldsymbol{E}}$(V/m) are quantities dependent on line elements. The magnetic flux density $\vec{\boldsymbol{B}}$(Wb/m^2), electric flux density $\vec{\boldsymbol{D}}$(Wb/m^2), current density $\vec{\boldsymbol{J}}$(A/m^2) are quantities dependent on surface elements. In order to conserve the conformal symmetry of the Maxwell's equations in the interior and exterior coordinates, permeability μ, permittivity ϵ, and conductivity σ are quantities which are defined by the quantities dependent on surface elements divided by the quantities dependent on line elements. Now, we introduce the metric defined by $g_i = \dfrac{h_j h_k}{h_i}$ in general curvilinear coordinates. The metric in spherical coordinate is given by (4). The schematic of the concept is shown in Fig. 2.

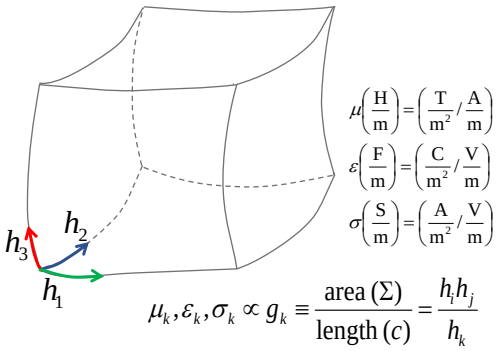

Fig. 2 Concept of the metric in general curvilinear coordinates

interior domain	exterior domain
$g_r = r^2\sin\theta$	$g'_r = -a^2\sin\theta$
$g_\theta = \sin\theta$	$g'_\theta = -\dfrac{a^2}{r^2}\sin\theta$
$g_\phi = \dfrac{1}{\sin\theta}$	$g'_\phi = -\dfrac{a^2}{r^2\sin\theta}$

(4)

$$\begin{aligned} \frac{\mu'_r}{\mu_r} &= \frac{\epsilon'_r}{\epsilon_r} = \frac{\sigma'_r}{\sigma_r} = \frac{\sigma^{*\prime}_r}{\sigma^*_r} = -\frac{g'_r}{g_r} = \frac{a^2}{r^2} \\ \frac{\mu'_\theta}{\mu_\theta} &= \frac{\epsilon'_\theta}{\epsilon_\theta} = \frac{\sigma'_\theta}{\sigma_\theta} = \frac{\sigma^{*\prime}_\theta}{\sigma^*_\theta} = -\frac{g'_\theta}{g_\theta} = \frac{a^2}{r^2} \\ \frac{\mu'_\phi}{\mu_\phi} &= \frac{\epsilon'_\phi}{\epsilon_\phi} = \frac{\sigma'_\phi}{\sigma_\phi} = \frac{\sigma^{*\prime}_\phi}{\sigma^*_\phi} = -\frac{g'_\phi}{g_\phi} = \frac{a^2}{r^2} \end{aligned} \tag{5}$$

The material constants of the Kelvin transformation can be derived by taking the ratio of the metric in the interior and exterior domains, and (5) are obtained. All the material constants are spatially modulated by $(a/r)^2$. Among various variable transformations, one of the advantages of using the Kelvin transformation is that it can treat the spatial modulation of the exterior domain as an isotropic material.

2.2 Finite Element Formulation

The A-, E-, and H-formulations are used in the high-frequency FEM. Among them, we employed the E-formulation, but the proposed method basically works with other formulations as well. On the boundaries of the interior and exterior domain, we imposed

$$\vec{\boldsymbol{n}} \times \vec{\boldsymbol{E}}_{in} = \vec{\boldsymbol{n}} \times \vec{\boldsymbol{E}}_{out} \tag{6}$$

as unknown-equivalent boundary conditions. We have employed a simple Maxwellian PML. The complex-relative permittivity $\epsilon_r^{\mathrm{PML}}$ and complex-relative permeability of the PML μ_r^{PML} must be the same values in a simple Maxwellian PML. In the extended Kelvin transformation method, the spherical Maxwellian PML

is at the center of the exterior domain, thus the effective thickness of the PML is large. The material properties of the PML in the exterior domain is spacially modulated by $(a/r)^2$, as given 5. They are the airbitrary functions of the radial component $r' = \sqrt{x'^2 + y'^2 + z'^2}$, as far as the imaginary part of $\mu_r^{\rm PML}$ and $\epsilon_r^{\rm PML}$ are sufficiently large for the radiating wave to decay.

In high-frequency problems, it is necessary to not only enlarge the analysis domain, but also absorb the incident waves and suppress the reflected waves. To achieve the absorbing boundary condition, we employ the PML [4–7] and place it in the exterior domain. The conventional PML is placed to surround the analysis domain, but the proposed method places it as a spherical shape at the center of the exterior domain. The PML assumes a characteristic impedance of 377 ohms, which is the impedance of spherical or plane waves, and therefore needs to be placed far enough from the wave source. For low-frequency problems, it is known that the PML must be thick enough to perform as a good absorber. These two requirements can be met relatively easily by using the Kelvin transformation. The PML of the proposed method has some flexibility in its implementation. With the proposed method, the material constants are moduled by the Kelvin transformation, but they can be simple Maxwellian unsplit PML because they are placed far enough from the electromagnetic sources.

3. Numerical Examples

Fig. 3 shows the numerical analysis model used for the verification of the proposed method. A Hertzian dipole with the frequency $f = 100$ MHz was placed offset in the x direction from the orign of the interior domain. A Perfect Electric Conductor (PEC) ground was placed at $z = -2$ m, and a dielectric scatterer was placed at a position 5 m away from the Hertzian dipole center in the x direction. The interior domain is truncated by a sphere of radius a and the ground plane. The scattering object outside the interior domain is Kelvin-transformed into the exterior domain. Since the plane is Kelvin-transformed to the sphere, the PEC ground becomes a part of the sphere, and the rectangular scattering object becomes a shape with a part of the sphere as a face. No mesh is generated in the region of radius 0.25 m at the center of the exterior domain to avoid the singularity, that can be assumed to be far enough from the electromagnetic source and in-between a PML is placed, therefore no electromagnetic wave approaches. The PML was placed at a distance of 8 m from the origin and Kelvin transformed in the exterior domain. The position of 8 m is larger than a, so it is Kelvin-transformed to a sphere of radius $a^2/8$ in the exterior domain. The complex-relative permittivity $\epsilon_r^{\rm PML}$ and complex-relative permeability of the PML $\mu_r^{\rm PML}$ are both $1 - 0.2$j. Since the wavelength of the electromagnetic wave at 100 MHz is 3 m, this is sufficiently far away. They are Kelvin transformed to

$$\epsilon_r'^{\rm PML} = \mu_r'^{\rm PML} = (1 - 0.2{\rm j})\frac{a^2}{r'^2}. \tag{7}$$

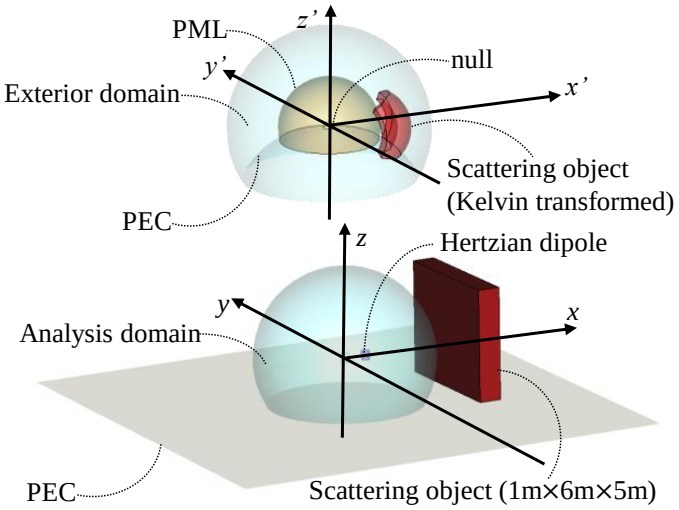

Fig. 3 Numerical analysis model used for the verification of the extended Kelvin transformation with PML.

3.1 Model without a scatterer

In this subsection, the relative permittivity ϵ_r and relative permeability μ_r are both $\epsilon_r = 1$ and $\mu_r = 1$, so that the model can be assumed to have no conductors and we can compare with the analytical solution. The analytical solution of the Herzian dipole is given by

$$E_r = \frac{Ile^{-jkr}}{j2\pi\omega\varepsilon_0}\left(\frac{1}{r^3} + \frac{jk}{r^2}\right)\cos\theta \tag{8}$$

$$E_\theta = \frac{Ile^{-jkr}}{j4\pi\omega\varepsilon_0}\left(\frac{1}{r^3} + \frac{jk}{r^2} - \frac{k^2}{r}\right)\sin\theta \tag{9}$$

where k is the wave number, r is the distance form the dipole, ω is the angular frequency, and ϵ_0 is the vacuum permittivity. We employed mirror image theory to consider the ground effect.

Fig. 4 and 5 show the contour plots the real and imaginary parts of the electric field E_θ, respectively. Fig. 6 shows the amplitude of the electric field E_θ along x-axis. The right figures are inside the interior domain and the left ones are in the exterior domain. The radius of the interior domain is set to $a = 4.0$ m and a Hertzian dipole is placed at $x_0 = 0$ m, $x_0 = 1$ m, and $x_0 = 2$ m. In order to compare them directly, the plots are shifted with the offsets. In every case, we could observe a good agreement with the analytical solution and consistent results with various offsets.

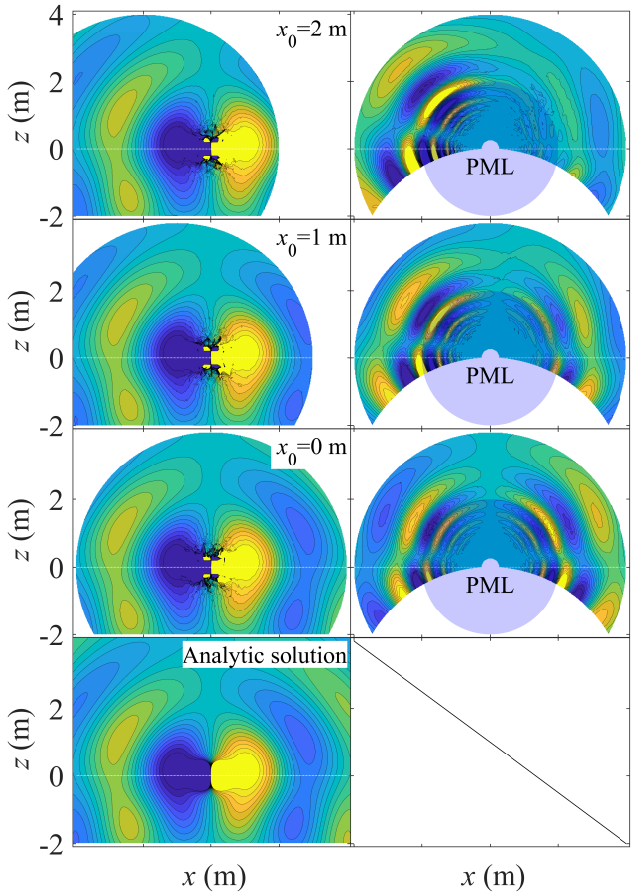

Fig. 4 Contour plots of the real part of the electric field in xz-plane without a scatterer. Left: interior domain, right: exteior domain.

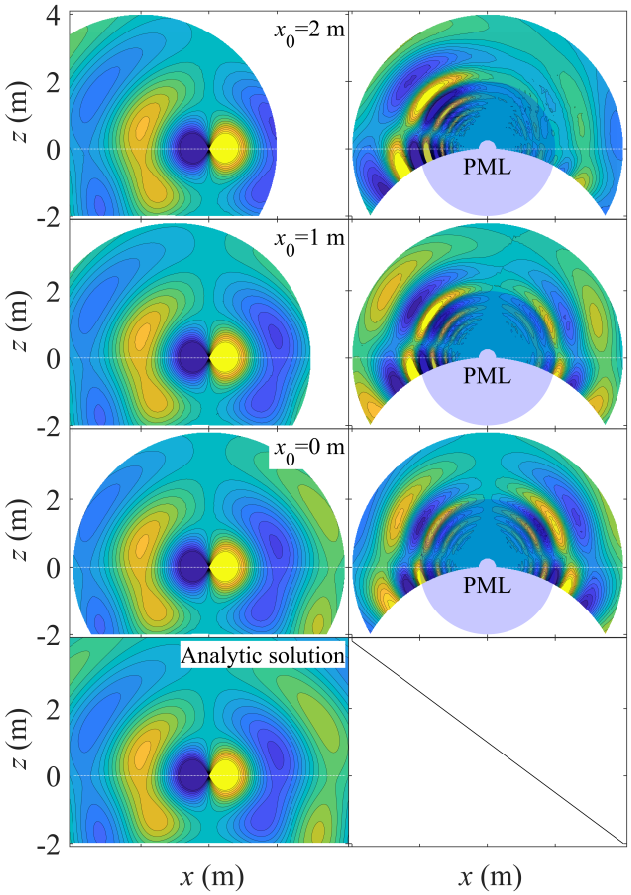

Fig. 5 Contour plots of the imaginary part of the electric field in xz-plane without a scatterer. Left: interior domain, right: exteior domain.

3.2 Model with a scatterer

In this example, the relative permittivity ϵ_r and relative permeability μ_r of the scatterer of 1 m $\times$ 6 m $\times$ 5 m are $\epsilon_r = 100 - 1000\mathrm{j}$ and $\mu_r = 1$, respectively, to verify the proposed method even with a scattering object in the exterior domain. Because the model does not have an analytical solution, we used a commercial MoM solver "FEKO", as a reference solution.

Fig. 7 and 8 show the contour plots and line plots of the real and imaginary parts of the electric field E_z, respectively. Fig. 9 shows the amplitude of the electric field E_θ along x-axis. The right figures are inside the interior domain and the left ones are in the exterior domain. The radius of the interior domain is set to $a = 2.5$ m, and $a = 4.0$ m, and a Hertzian dipole is placed at $x_0 = 0$ m with no offset. With our computer that has 128 GB of memory, we could not even calculate a model with $a \geq 5$ m. In every case, we could observe a good agreement with the reference solution and consisted results with various interior-domain size. However, there is no systematic discussion of accuracy with respect to the size of the analysis domain

and the external domain, which is highly dependent on the problem.

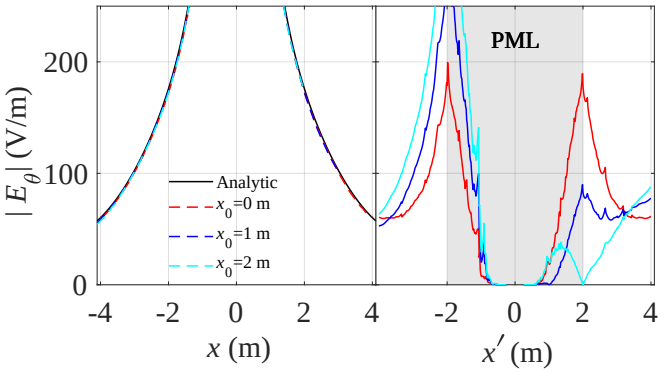

Fig. 6 Comparisons of the electric field along x-axis without a scatterer. Left: interior domain, right: exteior domain.

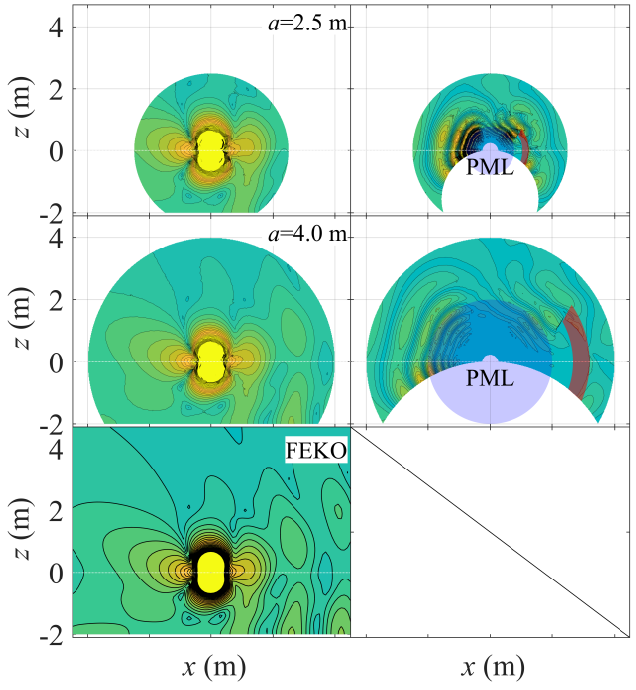

Fig. 7 Contour plots of the absolute values of the electric field in xz-plane with a scatterer. Left: interior domain, right: exteior domain.

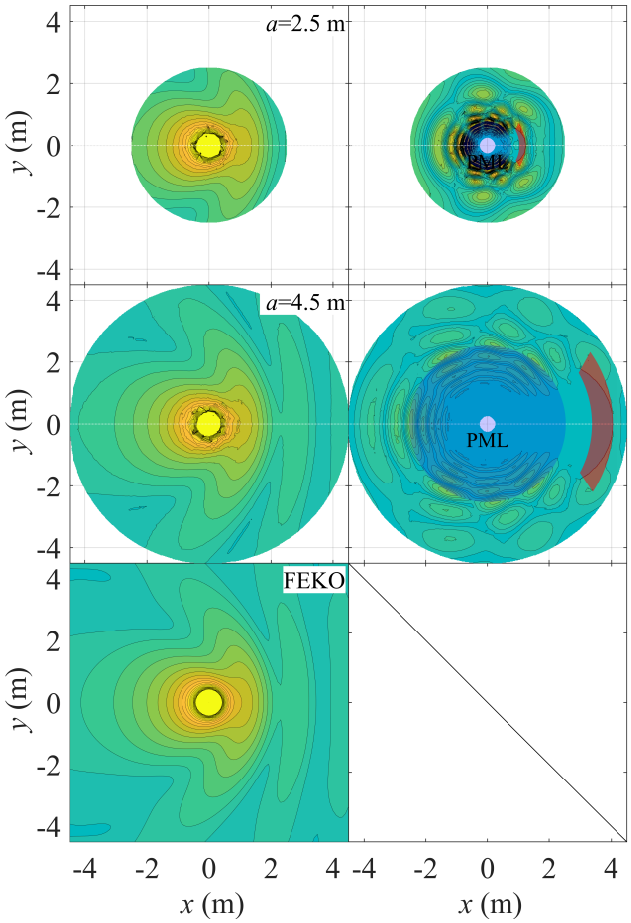

Fig. 8 Contour plots of the absolute values of the electric field in xy-plane with a scatterer. Left: interior domain, right: exteior domain.

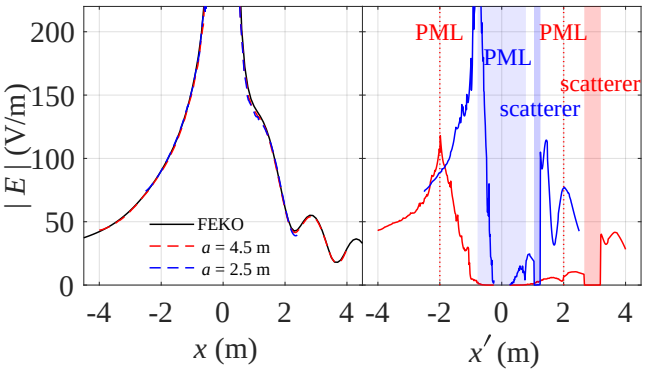

Fig. 9 Comparisons of the electric field along x-axis with a scatterer. Left: interior domain, right: exteior domain.

4. Conclusion

The idea of the Kelvin transformation has been extended to high-frequency radiation problems. The proposed method is effective in the following two cases: 1)

when surrounding scattering objects are present; and 2) when the radiating object is small compared to the wavelength and the thick PML is required. The numerical verification of the proposed method is performed with three-dimensional examples.

Acknowledgments

This work was supported by JSPS KAKENHI (Grant-in-Aid for Scientific Research (C)) Grant Number JP23K03826.

References

[1] Q. Chen and A. Konrad, "A review of finite element open boundary techniques for static and quasi-static electromagnetic field problems," *IEEE Transactions on Magnetics*, vol. 33, no. 1, pp. 663–676, 1997.

[2] R. Mittra, O. Ramahi, A. Khebir, R. Gordon, and A. Kouki, "A review of absorbing boundary conditions for two and three-dimensional electromagnetic scattering problems," *IEEE transactions on magnetics*, vol. 25, no. 4, pp. 3034–3039, 1989.

[3] G. Kriegsmann, A. Taflove, and K. Umashankar, "A new formulation of electromagnetic wave scattering using an on-surface radiation boundary condition approach," *IEEE Transactions on Antennas and Propagation*, vol. 35, no. 2, pp. 153–161, 1987.

[4] J.-P. Berenger, "A perfectly matched layer for the absorption of electromagnetic waves," *Journal of Computational Physics*, vol. 114, no. 2, pp. 185–200, 1994.

[5] A. B. G. S. N. Alfonzetti, S., "Some considerations about the perfectly matched layer for static fields," *COMPEL - The international journal for computation and mathematics in electrical and electronic engineering*, vol. 18, no. 3, pp. 337–347, 1999.

[6] J. A. Roden and S. D. Gedney, "Convolution pml (cpml): An efficient fdtd implementation of the cfs pml for arbitrary media," *Microwave and Optical Technology Letters*, vol. 27, no. 5, pp. 334–339, 2000.

[7] L. Dedek and J. Dedkova, "Optimization of perfectly matched layer for laplace's equation."

[8] E. Becache, P. Petropoulos, and S. Gedney, "On the long-time behavior of unsplit perfectly matched layers," *IEEE Transactions on Antennas and Propagation*, vol. 52, no. 5, pp. 1335–1342, 2004.

[9] O. Ozgun and M. Kuzuoglu, "Non-maxwellian locally-conformal pml absorbers for finite element mesh truncation," *IEEE Transactions on Antennas and Propagation*, vol. 55, no. 3, pp. 931–937, 2007.

[10] J. P. Webb, "Application of the finite-element method to electromagnetic and electrical topics," *Reports on Progress in Physics*, vol. 58, no. 12, p. 1673, dec. [Online]. Available: https://dx.doi.org/10.1088/0034-4885/58/12/002

[11] S. Wong and I. Ciric, "Method of conformal transformation for the finite-element solution of axisymmetric exterior-field problems," *Compel*, vol. 4, no. 3, pp. 123–135, 1985.

[12] I. Ciric and S. Wong, "Inversion transformation for the finite-element solution of three-dimensional exterior-field problems," *COMPEL-The international journal for computation and mathematics in electrical and electronic engineering*, 1986.

[13] E. Freeman and D. Lowther, "A novel mapping technique for open boundary finite element solutions to poisson's equation," *IEEE Transactions on magnetics*, vol. 24, no. 6, pp. 2934–2936, 1988.

[14] ——, "An open boundary technique for axisymmetric and three dimensional magnetic and electric field problems," *IEEE Transactions on Magnetics*, vol. 25, no. 5, pp. 4135–4137, 1989.

[15] D. Lowther, E. Freeman, and B. Forghani, "A sparse matrix open boundary method for finite element analysis," *IEEE Transactions on Magnetics*, vol. 25, no. 4, pp. 2810–2812, 1989.

[16] D. Y. Zhang Fanga, Tang Zhanghongb and Y. Jianshenga, "Calculation of electrostatic field in 3-d unbounded non-uniform domains by fem with kelvin transformation," *International Journal of Applied Electromagnetics and Mechanics*, vol. 33, no. 1-2, pp. 307–312, 2010.

[17] K. Sugahara, "Periodic image method for open boundary axisymmetrical magnetic field problems," *IEEE transactions on magnetics*, vol. 49, no. 11, pp. 5399–5403, 2013.

[18] A. A. M. Farah, M. M. Afonso, J. A. Vasconcelos, and M. A. O. Schroeder, "A finite-element approach for electric field computation at the surface of overhead transmission line conductors," *IEEE Transactions on Magnetics*, vol. 54, no. 3, pp. 1–4, 2018.

[19] G. Gold, "On the kelvin transformation in finite difference implementations," *Electronics*, vol. 9, no. 3, 2020. [Online]. Available: https://www.mdpi.com/2079-9292/9/3/442

[20] D. Meeker, "Improvised open boundary conditions for magnetic finite elements," *IEEE transactions on magnetics*, vol. 49, no. 10, pp. 5243–5247, 2013.

[21] D. C. Meeker, "Improvised asymptotic boundary conditions for electrostatic finite elements," *IEEE transactions on magnetics*, vol. 50, no. 6, pp. 1–9, 2014.

[22] K. Sugahara, "Improvised asymptotic boundary conditions for magnetostatic field problems in ellipsoidal and elliptic cylindrical domains," *IEEE Transactions on Magnetics*, vol. 53, no. 6, pp. 1–4, 2017.

[23] ——, "Improvised absorbing boundary conditions for three-dimensional electromagnetic finite elements," pp. 1094–1097, 2015.

[24] ——, "Electromagnetic analysis of wireless power transfer system with improvised absorbing boundary conditions," pp. 1152–1155, 2016.

[25] O. Kellogg, *Foundations of Potential Theory*, ser. Die Grundlehren der mathematischen Wissenschaften in Einzeldarstellungen. Dover Publications, 1953. [Online]. Available: https://books.google.co.jp/books?id=TxlfQi46CvEC

[26] W. Thomson, "Extrait d ' une Lettre de M. William Thomson à M. Liouville."

[27] G. Dassios and R. E. Kleinman, "On Kelvin inversion and low-frequency scattering," *SIAM Review*, vol. 31, no. 4, pp. 565–585, 1989. [Online]. Available: https://doi.org/10.1137/1031126

[28] M. S. Nabizadeh, R. Ramamoorthi, and A. Chern, "Kelvin transformations for simulations on infinite domains," *ACM Transactions on Graphics (TOG)*, vol. 40, no. 4, pp. 97:1–97:15, 2021.

[29] K. Sugahara, "Electromagnetic analysis of eddy current testing with Kelvin transformation," *IEEE Transactions on Magnetics*, vol. 58, no. 9, pp. 1–6, 2022.

[30] L. Yeh, "Conformal transformation and Maxwell's equations," Nov. 2023, working paper or preprint. [Online]. Available: https://hal.science/hal-04281513

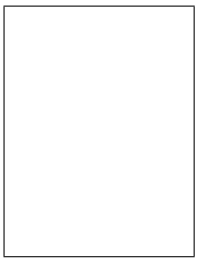

Kengo Sugahara received the B.A. degree in physics from Keio University, Kanagawa, Japan in1999, and the M.A. degree in physics from Kyoto University, Kyoto, Japan in 2001. He has received the Ph. D. degree from Hosei University, Tokyo, Japan in 2007. During 2001–2014 he worked for Mitsubishi Electric Corporation as a research engineer in the applied magnetics group He is now a associate professor in Kindai University.